Construction and Building Materials 145 (2017) 243–252

Contents lists available at ScienceDirect

Construction and Building Materials

journal homepage: www.elsevier.com/locate/conbuildmat

Using glass sand as an alternative for quartz sand in UHPC

Nancy A. Soliman, Arezki Tagnit-Hamou *

HIGHLIGHTS

- Valorization of waste glass in concrete saves its landfills and reduce concrete price.
- GS with mean particle size 275 μm can be used to replace QS in UHPC.
- GS as QS replacement can yield a UHPC with a dense microstructure.
- GS as QS replacement can yield a UHPC without any expansion from alkali–silica reaction.

ARTICLE INFO

Article history:
Received 15 April 2016
Received in revised form 16 March 2017
Accepted 25 March 2017
Available online 9 April 2017

Keywords:
Ultra-high-performance concrete
Glass sand
Quartz sand
Packing density
Mechanical properties
Microstructure
Alkali–silica reaction

ABSTRACT

Ultra-high-performance concrete (UHPC) is characterized by a dense microstructure that yields ultra-high strength and durability properties. Quartz sand (QS) with maximum particle sizes of 600 μm represents the coarse particles in (UHPC). The QS with optimum grading curve is obtained from crushing coarse sand or rocks, however this is a time-consuming, costly, and polluting process. This paper reports on a study to determine the possibility of producing and using glass sand (GS) for partial or total replacement of QS in UHPC. The results show that GS with a mean particle size (d_{50}) of 275 μm could be recommended as an optimal PSD to replace QS particles. The results demonstrate that compressive strength values of about 196 and 182 MPa after two days of hot curing can be achieved when replacing 50% and 100% of QS with GS, respectively, compared to 204 MPa for reference UHPC containing 100% QS. Incorporating higher replacement rates of GS was shown to produce UHPC of accepted flowability and dense microstructure that mitigated the aggregate alkali–silica reaction.

© 2017 Elsevier Ltd. All rights reserved.

1. Introduction

Large quantities of glass cannot be recycled because of high breaking potential, color mixing, or high recycling costs [1]. Most waste glass is routinely disposed of in landfill sites, which is undesirable as it is not biodegradable and not environmentally friendly [2]. As awareness has grown about the need to protect the environment, attention has increasingly focused on turning solid waste into concrete ingredients. Apart from the savings in terms of material and energy resources, reusing some solid wastes could result in better concrete performance in several areas. Fine ground glass particles (smaller than 75 μm) can exhibit pozzolanic reactivity, thereby improving the paste microstructure as well as the concrete's long-term strength and durability [3–4]. Studies have been conducted to determine the pozzolanicity of GP concrete, revealing that the GP's pozzolanic activity depends on its fineness. Moreover, the pozzolanic reaction takes place at a slower rate at early age, and then accelerates at later age compared to cement hydration [5–16]. Furthermore, no alkali–silica reaction has been observed with finely ground glass powder (GP) [17].

Waste glass has been used as coarse and fine aggregates in concrete, because of its much lower absorption and similar density (2.60) to natural gravel and sand [18]. Better mechanical results were observed when replacing natural sand with glass sand (GS) (finer than 5 mm), since the texture properties of the glass particles can be improved by reducing the particle size. Park et al. [19] measured approximately similar compressive strength (f'_c) (only 1% lower), and splitting-tensile (f_{st}) and flexural (f_{fl}) strengths (only 3% lower) for concrete containing 30% GS as sand replacement compared to the control concrete. At higher replacement levels, they also noticed that the GS did not significantly affect the strength. The authors suggested that this slightly lower strength was due to lower adhesion between the cement and glass than between the cement and natural sand, which is probably due to the lower absorption of the glass. In Turgut and Yahlizade's study [20] on producing paving blocks, the 20% replacement of sand with GS resulted in significant increases in the f'_c, f_{st}, f_{fl}, and abrasion resistance of 69%, 47%, 90%, and 15% compared to control, respec-

* Corresponding author.
E-mail address: A.Tagnit@USherbrooke.ca (A. Tagnit-Hamou).

http://dx.doi.org/10.1016/j.conbuildmat.2017.03.187
0950-0618/© 2017 Elsevier Ltd. All rights reserved.

tively. The authors attributed these increases to the GS's pozzolanic nature.

Since glass has very low absorption, the water absorption of the concrete containing GA can be greatly reduced, thereby potentially improving the concrete's durability [21]. Low water absorption was also observed for the paving blocks made with waste GA [20].

While the above investigations demonstrate that waste glass can be used as an aggregate in concrete, its applications are limited due to the damaging expansion in the concrete caused by alkali–silica reaction (ASR) between the high-alkali pore water in cement paste and the reactive silica in the waste glass. The chemical reaction between the alkali in portland cement and silica in the aggregate forms silica gel that not only causes cracks upon expansion, but also weakens the concrete and shortens its life. Jin et al. [17] reported that glass with particle sizes ranging from 1.18 to 2.36 mm produced the highest expansion, whereas low expansion was observed with larger and smaller particle sizes. Idir et al. [22] reported that glass particles larger than 1 mm produced ASR gel, but smaller particles produced C-S-H through pozzolanic reaction. Indeed, when the particles are slightly less than 1 mm, a nonexpansive local ASR gel forms around the particles, leading to better bonding between the particles and the cement paste [22]. Some of the common methods to reduce the deterioration associated with ASR are to use low-alkali cement, or use supplementary cementitious materials, or prevent water from entering the concrete [23], or treat the aggregates with admixtures [23,24]. A fly-ash content of 20% of the total binder content greatly reduces the ASR expansion resulting from glass aggregate in the concrete [25]. Lam et al. [26] reported that 10% fly ash used in the concrete can prevent ASR damage in paving blocks containing GA. Shayan and Xu [1] found that both 10% silica fume (SF) and more than 20% GP as a cement replacement were able to ensure no negative ASR expansion in mortar bars.

With recent developments in concrete technology, new generations of concrete have been produced, such as ultra-high-performance concrete (UHPC). The UHPC is defined worldwide as concrete with high mechanical, ductility, and durability properties [27]. Typical UHPC mix designs consist of very high cement content, SF, quartz powder (QP), quartz sand (QS), and steel fiber [28]. The fiber inclusion in UHPC improves the material's ductility and flexural capacity. With UHPC, a f'_c greater than 150 MPa, a f_{fl} of up to 15 MPa, an elastic modulus (E_c) of 45 GPa, and minimal long-term creep can be achieved [28,29]. The UHPC can also resist freeze–thaw cycles and deicing-salt scaling without any visible damage, and it is nearly impermeable to chloride-ion penetration [30–32]. These excellent characteristics of UHPC are achieved by enhancing homogeneity, eliminating the coarse aggregate, enhancing packing density, improving microstructure, and including fiber [27,28]. Currently, UHPC is used in the construction of special prestressed and precast concrete elements, such as decks and abutments of lightweight bridges, marine platforms, precast walls, concrete repair, urban furniture, and other architectural applications [33–36].

Meeting the optimum grading requirement of QS (in the range of 150–600 μm), for homogeneity and optimum packing density of the UHPC matrix is one of the challenges in producing UHPC. In absence of the QS with the required optimum grading, it is common to obtain the grading by crushing coarse sand or rocks, which is time-consuming, costly, and polluting due to dust generation during crushing. Based on an Environment Canada report [37], quartz dust causes immediate and long-term environmental harm because its biological diversity makes it an environmental hazard. Additionally, the International Agency for Research on Cancer (IARC) has classified respirable quartz due to occupational exposure as a Group 1 carcinogen (carcinogenic to humans). The U.S. National Toxicology Program has classified crystalline silica of respirable size as a human carcinogen. The basis for these classifications is sufficient evidence from human studies, indicating a causal relationship between exposure to respirable crystalline silica in the workplace and increased lung-cancer rates in workers [38]. Based on this information, an intensive effort to replace QS with other safe, harmless materials should be undertaken. Even though UHPC is an innovative durable material, it contains a large amount of natural QS. Replacing this sand with GS can significantly decrease its environmental impact.

The current research project aimed at producing UHPC with GS as a partial or total replacement of QS. The effect of QS replacement was studied by measuring the packing density of concrete, fresh properties, compressive strength, ASR, and microstructure. The effect of normal- and steam-curing conditions on the compressive-strength properties was considered.

2. Research significance

Sustainable development for construction involves using unconventional and innovative materials or reusing waste materials in order to compensate for the lack of natural resources and to find alternative ways for conserving the environment. Replacement of quartz sand (QS) in the UHPC mix design with glass sand (GS) derived from crushing waste-glass cullets could decrease the use of QS, whose costly, and environmentally hazardous. Replacing QS with GS can reduce dramatically the price of conventional UHPC by reducing the QS content or avoiding the transportation costs associated with QS when using locally available GS to produce UHPC. By incorporating GS as a replacement of QS in UHPC, environmental hazards and human carcinogenic risks associated with the grinding of quartz could be avoided. Waste glass that is not biodegradable can be reused in concrete, so less material has to be stockpiled or placed in landfills.

3. Experimental program

The key parameter for developing UHPC is to avoid using coarse aggregate and sand with large particle sizes that are normally used in the mix design of normal concrete (NC) and high-performance concrete (HPC), and replace them with ground quartz with particle sizes less than 600 μm [27]. Consequently, the weak transition zone at the interface between the aggregates and paste in NC and HPC can be attenuated, leading to maximum packing density and performance enhancement. Therefore, the coarser material used in conventional UHPC is QS with maximum particle sizes of less than 600 μm. Consequently, the main purpose of optimizing the grading (PSD) of the GS is to make it as close to that of QS as possible to arrive at a particular combination of granular materials, which can yield optimum packing density.

To obtain an optimum packing density for GS, the crushed GS was first separated into three grades similar to standard sand size fractions; grade 1 (320 μm < GS1 < 630 μm) coarse, grade 2 (160 μm < GS2 < 320 μm) medium, and grade 3 (80 μm < GS3 < 160 μm) fine. The packing densities of unitary, binary, and ternary combinations were computed based on the Sedran and De Larrard approach [39,40] to obtain the optimum packing density of GS. Based on the packing density results, three sets of ternary combinations (the highest packing density) among GS1, GS2, and GS3 were selected. The three sets had PSDs with mean particle sizes (d_{50}) of 225, 275, and 350 μm, and were used to replace 100% of the QS in conventional UHPC. This was to select the optimum GS combination, not only based on the highest packing density, but also on producing optimum concrete properties (workability and compressive strength).

The best GS combination in terms of both packing density and concrete properties was then used with different QS replacements (0%, 50%, and 100%). The relevant effect of QS replacement in UHPC was studied in terms of concrete packing density, workability, mechanical properties, ASR, and microstructure.

The effect of two different curing conditions—normal curing (NC) at a temperature (T) of 20 ± 2 °C and relative humidity (RH) of 100%, and standard steam hot curing (HC) at T = 90 °C and RH = 100% for 48 h—was considered as a parameter affecting the compressive-strength properties of UHPC mixtures.

The mix-design optimization method, mixture composition, material properties, and test methods undertaken in this research are detailed in the following sections.

3.1. Materials characterization

The C_3A and C_3S contents and fineness of cement are critical to control concrete rheology [41]. This is more pronounced with UHPCs designed with higher cement contents. Therefore, high sulfate-resistant cement (Type HS cement) with low C_3A and C_3S contents was selected for designing the UHPC mixtures. The SF used in the mixture proportioning complies with CAN/CSA A3000 specifications [42]. The UHPC was also designed with QS with a specific gravity (SG) of 2.70 and a maximum particle diameter (d_{max}) of 600 μm. The QP with a SG of 2.73 and d_{50} of 13 μm was used as a filler material. The waste glass material with a d_{max} of 600 μm is referred as GS. The GS had a silica content of 73% and Na_2O content of 13%. Its SG was 2.60. Table 1 provides the chemical and physical properties of the type HS cement, SF, QS, QP, and GS materials. The physical properties included material SG, Blain surface fineness, d_{50}, and d_{max}. Fig. 1 provides the single PSD for the Type HS cement, QP, SF, and QS as well as the PSD of the combined granular materials in the UHPC. The micrographs in Fig. 2 show the morphology and size of particles for both QS and GS. The XRD analysis indicates that the QS is crystallized, while the GS is amorphous, as shown in Fig. 3. A polycarboxylate (PCE)-based high-range water-reducing admixture (HRWRA) with a SG of 1.09 and solid content of 40% was used in all the concrete mixtures.

The costs for each UHPC constituent is listed in Table 1. The materials are obtained from reputable suppliers and the costs specified are valid for 2014 when the bulk of the research was conducted.

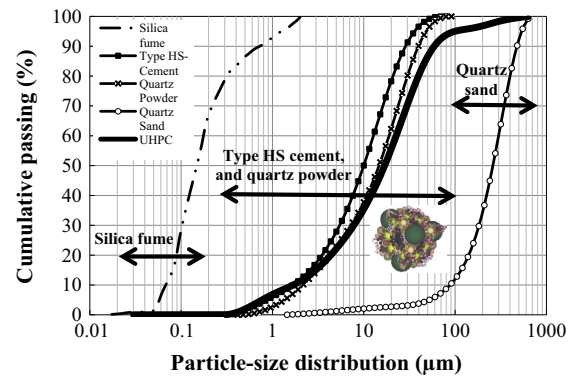

Fig. 1. Particle-size distributions of individual and combined granular materials used in the UHPC reference-mix design.

3.2. Mix-design optimization and mixture composition

UHPC development starts with designing the granular structure of all the granular components. The key factor for enhancing UHPC performance is optimizing the particle-size distribution and packing density. The granular structure strongly affects the balance between the UHPC rheological behavior and mechanical performances. In this research, the design of the granular structure of the UHPC (reference mixture in Table 2) was made using the compressible packing model (CPM) developed by De Larrard and collaborators [39,40]. Fig. 1 shows the PSDs for all single materials and the combined materials to produce the reference UHPC mixture (Table 2). The water-to-binder ratio (w/b) of 0.189 and HRWRA dosage of 1.5% (% wt. of solids to cement weight) were used, which were obtained by optimizing the different UHPC mixtures carried out in a previous study [35].

The other five UHPGC mixtures in Table 2 were designed based on the reference UHPC mixture by taking into account the QS replacement with GS on a weight basis. The three mixtures (0QS/100GS-350, 0QS/100GS-275, and 0QS/100GS-225) in Series I contained GS with different PSDs (d_{50} of 350, 275, and 225 μm, respectively) as total QS replacement. Based in the results of the concretes in Series I, an optimum GS was selected to produce the concretes in Series II. In both mixtures in Series II, 50% and 100%

Table 1
Chemical composition (%) of Type HS cement, quartz sand, quartz powder, glass powder, and silica fume.

	Identification	Quartz Sand	Quartz Powder	Glass Sand-0.60	HS Cement	Silica Fume
Chemical composition (%)	Silicon dioxide (SiO_2)	99.80	99.80	73.00	22.00	99.80
	Iron oxide (Fe_2O_3)	0.04	0.09	0.40	4.30	0.09
	Aluminum oxide (Al_2O_3)	0.14	0.11	1.50	3.50	0.11
	Calcium oxide (CaO)	0.17	0.38	11.30	65.6	0.40
	Titanium dioxide (TiO_2)	0.02	0.25	0.04	0.20	–
	Sulfur trioxide (SO_3),	–	0.53	–	2.30	–
	Magnesium oxide (MgO)	0.01	0.20	1.20	1.90	0.20
	Sodium oxide (Na_2O)	–	0.25	13.00	0.07	0.20
	Potassium oxide (K_2O)	0.05	3.50	0.50	0.80	0.50
	Equivalent alkali (Na_2O_{eq})	–	–	–	0.90	–
	Zinc oxide (ZnO)	–	–	–	0.09	0.25
	Loss on ignition (LOI)	0.20	0.32	0.60	1.00	3.50
Bogue components	C_3S	–	–	–	50.00	–
	C_2S	–	–	–	25.00	–
	C_3A	–	–	–	2.00	–
	C_4AF	–	–	–	14.00	–
Physical properties	Specific gravity	2.70	2.73	2.60	3.21	2.20
	Blaine surface area (m^2/kg)	–	–	–	430	20,000
	Mean particle diameter, d_{50}, (μm)	250	13	270	11	0.15
	Maximum particle diameter, d_{max}, (μm)	600	–	630	–	–
	Cost ($/ton)	235	560	50	220	450

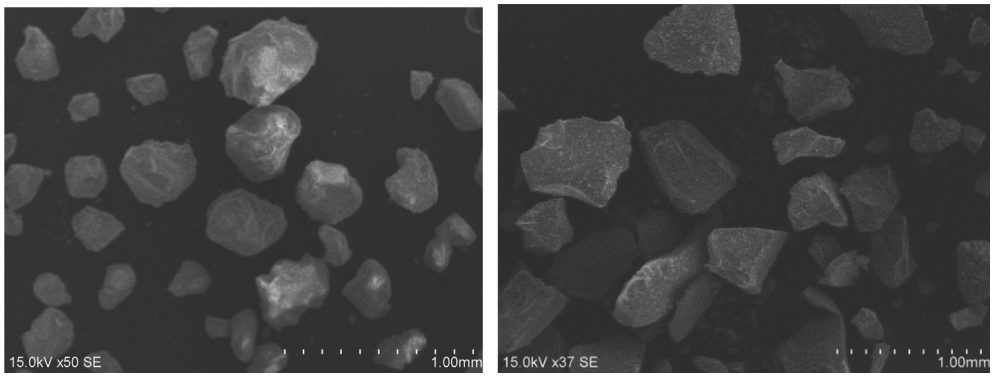

Fig. 2. Photomicrograph of quartz sand (left) and glass sand (right).

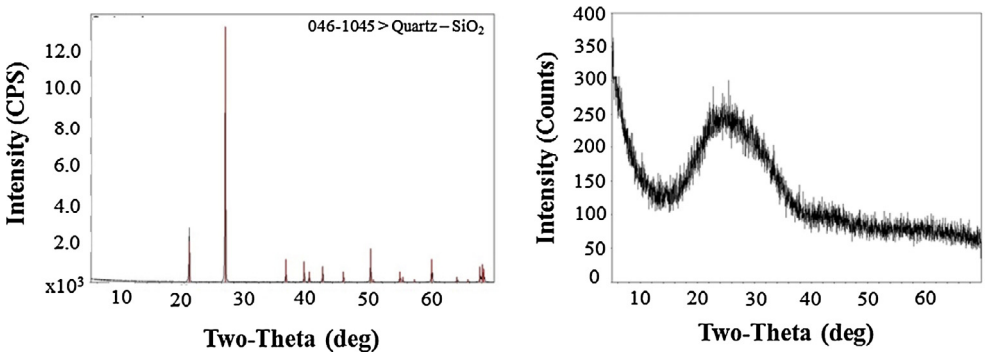

Fig. 3. X-ray diffraction patterns for quartz sand (left) and glass sand (right).

Table 2
Concrete mix design (kg/m^3).

Material	Reference	Series I (100% replacement of QS with GS with different PSDs)			Series II (QS replacement with GS with optimum granulometry (d_{50} = 275 μm)	
		0QS/100GS-350	0QS/100GS-275	0QS/100GS-225	50QS/50GS	0QS/100GS
Type HS cement	807	794	794	794	802	794
Silica fume	225	221	221	221	223	221
Water	196	192	192	192	194	192
Water-to-binder ratio *(w/b)*	0.189	0.189	0.189	0.189	0.189	0.189
Quartz sand	972	–	–	–	481	–
Glass sand (GS-350)	–	953	–	–	–	–
Glass sand (GS-275)	–	–	953	–	481	953
Glass sand (GS-225)	–	–	–	953	–	–
Quartz powder	243	238	238	238	241	238
Solid content in HRWRA	13	13	13	13	13	13
Normalized cost index relative to reference mixture ($/$)	1.00	0.84	0.84	0.84	0.92	0.84

of the QS content in the reference mixture were replaced with the optimum GS from Series I (d_{50} = 275 μm). The cement, SF, QP, *w/b*, and HRWRA contents were kept constant in all the concrete mixtures.

The names of the mixtures in Series I are combination of QS percentage and GS percentage. The number next to GS represents the d_{50} of the GS used in the mixture. For example, the 0QS/100GS-350 mixture had 0% of QS and 100% of GS with a d_{50} of 350 μm. In Series II, only the replacement ratios of both the QS and GS were used, with adding a value for the d_{50} because the two mixtures in this series were made with same GS (d_{50} = 275 μm).

Table 2 shows the materials cost (represented as normalized *cost index*) for all concrete mixtures considered in this work. The normalized *cost index* is calculated as the ratio between a given mixture's cost to the cost of the reference mixture, based on recent prices in Canada. The *cost index* is a relative indicator of cost, since the actual cost varies based on time and location.

3.3. Testing procedures

All the concrete mixtures were batched using high-energy shear mixer with a 10 L capacity. To achieve a homogeneous mixture and avoid particle agglomeration, all of the powdered materials were mixed for 10 min before water and HRWRA addition. Approximately half of the HRWRA diluted in half of the mixing water was gradually added over 5 min of mixing time. The remaining water and HRWRA were gradually added over an additional 5 min of mixing time. Upon the end of mixing, the fresh properties

of the UHPC mixtures were measured. The fresh tests included concrete temperature, unit weight, and air content (ASTM C 185 [43]). The concrete flow was also measured using the mini-slump cone and flow table (ASTM C 1437 [44]).

The compressive strength (f_c) measurements for the UHPC were determined using 50 × 50 × 50 mm cubes, according to ASTM C 109 [45]. The samples were tightly covered with plastic sheets and stored at 23 °C and 50% RH for 24 h before demolding. After demolding, the samples were cured under two different curing regimes: NC and HC. Under NC, the samples were stored in a fog room at a temperature of 23 °C and 100% RH until the day of testing. The HC mode composed of curing the samples at 90 °C and 100% RH for 48 h before testing. Measurement of ASR expansion and mass variations over time were carried out for 50QS/50GS according to ASTM C1260 [46]. Standard mortar-bar molds (20 × 20 × 275 mm) were used to cast the specimens for this series of tests. Because this UHPC contained no coarse aggregate, no special preparation of the batch ingredients was necessary before casting the bars. Four prisms were cast with the concrete mixture and remained tightly covered with plastic sheets in molds at 23 °C and 50% RH for 24 h, before demolding. The first readings of length and mass changes were taken immediately after demolding. The specimens were immersed in a tap-water bath and then stored at 80 °C for 24 h before measuring the "zero" readings of length and mass. The samples were then immersed in a NaOH solution and stored again at 80 ± 2 °C. The mass and length changes were subsequently measured daily for a total of 14 days of saturation in the NaOH solution.

Additional samples from the reference (after HC treatment) and 50QS/50GS concretes after finishing the ASR test were also prepared for microstructure analysis using scanning electron microscope (SEM: Hitachi S-3400 N) coupled with energy dispersive spectroscopy (EDS: Oxford Inca). The SEM was operated at a pressure of 50 Pa, a voltage of 20 kV, and tungsten filament current of 80 μA. The SEM observations were performed on polished surfaces, from which a chunk of the concrete was removed and cast in resin. The cast samples was cut perpendicularly to its cross section and polished with a 1.0-μm roughness polishing pad. In this paper, each site of interest is presented with two SEM micrographs.

The packing density was measured for the GSs of different of PSD greater than 125 μm using the intensive-compaction-test (ICT) setup. The ICT machine consisted of a turntable and a cylinder exerting a pressure ranging between 20 and 1000 kPa over a certain number of cycles on the tested sample until the maximum density is reached [47]. In our study, the applied pressure was 20 kPa to avoid crushing the GS particles. If the GS sample with a weight (w) and a specific gravity (SG) fills up the ICT container with a volume (V_c), then the packing density (φ) can be calculated, as in Eq. (1), where V_s is the solids volume:

$$\phi = \frac{V_s}{V_c} = \frac{w}{V_c \cdot SG} \quad (1)$$

4. Results and discussions

4.1. Optimizing PSD of glass sand in UHPC using packing density

The packing densities of unitary, binary, and ternary combinations were computed based on the approach in [39]. Initially, the unitary packing density of each individual material was determined. The intensive-compaction-test (ICT) method was used for measuring the dry packing density of the GS with a PSD greater than 125 μm. The results of the unitary packing density for each of the three glass sands—GS1 (PSD = 320–630 μm), GS2 (PSD = 160–320 μm), and GS3 (PSD = 80–160 μm)—were 0.56, 0.55, and 0.50, respectively. The unitary packing of GS1 and GS2 were slightly higher than of GS3. According to [39,40], this could be attributed to the coarse friction being more amenable to compaction due to fewer contact points between grains than in the finer fraction.

The packing density of the binary combination between the two finer GSs (GS1 and GS2) was then determined, as shown in Fig. 4 (left). In general, the binary mixture showed higher packing density than the unitary packing. This was obviously due to the filling of void spaces with the finer particles. Adding GS2 to GS1 increased the packing up to 80% of GS2 and 20% of G1; after that point, the packing density started to decrease. The combination of 60% GS1 and 40% GS2 yielded the highest packing density of 0.60.

Ternary combinations among GS1, GS2, and GS3 were initially estimated by taking five binary mixtures between GS1 and GS2 (GS1 ranging from 80% to 40% and GS2 ranging from 20% to 60%, both in increments of 10%). For each ternary GS1- GS2, GS3 was added as a finer material in increments of 10% between 0% and 100% (see Fig. 4 [right]). The highest packing density value of 0.63 was achieved for two ternary GS1:GS2:GS3 combinations of 49%:21%:30% and 56%:24%:20%. The results show that adding GS3 at percentages between 10% and 50% increased the packing density of the granular materials by filling the gaps between the coarser materials in the binary mixtures.

While higher packing density is preferred, the maximum packing density may not be optimal [39]. When all the concrete particles are completely packed, the resultant concrete will have poor workability and be difficult to place. For practical purposes, fresh concrete needs to be placed and has to flow at least to a certain degree. Therefore, three sets of ternary combinations GS1:GS2:GS3 with packing-density values close to the maximum (0.63) were selected to study their effect on fresh properties and compressive strength in conventional UHPC. These three sets had percentages of 56%:24%:20%, 35%:35%:30%, and 36%:54%:10% with packing density values of 0.63, 0.62, and 0.60, respectively. Fig. 5 gives the PSDs for these three GS combinations with d_{50} values of 350, 275, and 225 μm, respectively. According to their respective d_{50} values, they were designated as GS-350, GS-275, and GS-225, respectively.

4.2. Effect of different PSD of glass sand on UHPC properties

Table 3 presents the fresh concrete temperature, unit weight, air content, and mini-slump flow values of the UHPC mixtures in Series I (containing GS with different PSD) compared to the reference mixture. Replacing the QS with GS-350 and GS-225 led to a decrease in workability. The slump flow decreased from 190 mm for the reference mixture to 175 and 170 mm in 0QS/100GS-350 and 0QS/100GS-225, respectively. The incorporation of GS-275 in the UHPC increased the slump flow to 210 mm in 0QS/100GS-275, compared to 190 mm in the reference.

The particle packing density of the concrete decreased when GS-350 and GS-225 were incorporated, compared to the reference mixture. For example, the packing-density values obtained from the CPM for the reference, 0QS/100GS-350, and 0QS/100GS-275 mixtures were 0.79, 0.76, and 0.75, respectively. This was attributed to the increased content of finer particles (80 to 160 μm) in GS-350 and GS-275, which decreased the concrete's workability. This resulted in an overlapping of the cement and QP particles, on the one hand, and the finer particles in GS3, on the other hand. In contrast to GS-350 and GS-225, including GS-275 in the UHPC—with a slightly lower particle packing density (0.78) due the decreased content of finer materials in GS3—resulted in improved concrete workability. In addition, the improvement in the flow characteristics reported for 0QS/100GS-275 compared to the reference mix-

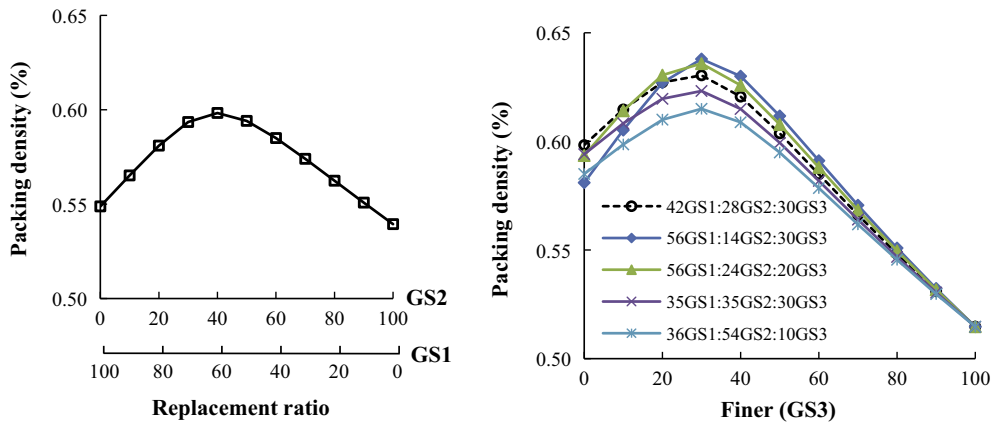

Fig. 4. Binary packing between GS1 and GS2 (left), ternary packing between the optimum combination between GS1 and GS2 against GS3 (right).

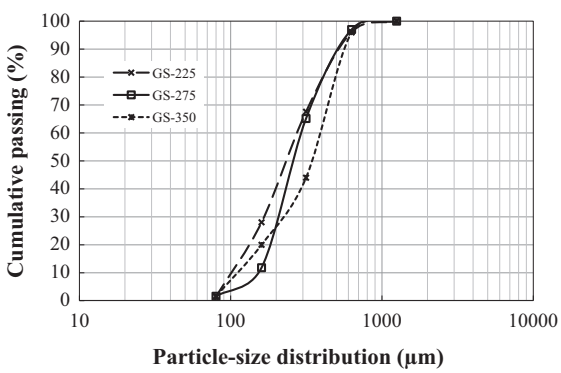

Fig. 5. Particle-size distributions for the three combinations of glass sand.

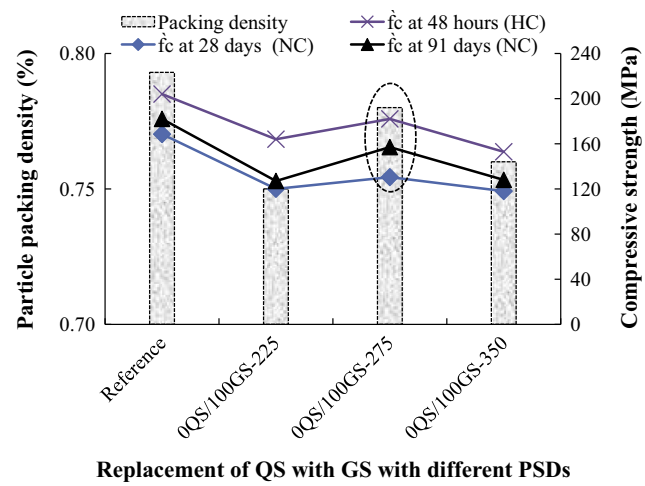

Fig. 6. Particle-packing density and compressive strength of UHPC mixtures made with glass sand (GS) with different particle-size distributions (PSDs).

ture was due replacing QS particles in the latter mixture with GS particles with low water absorption and smooth surfaces.

The unit weight of the reference mixture remained close to that of the concretes containing the three different GSs, given that the SG value of the QS was not far from that of the GS (2.75 vs. 2.60, respectively), as seen in Table 1.

Compared to the reference mixture made with only QS, the three mixtures containing GS in Series I showed relatively higher air contents. For example, 0QS/100GS-350 with GS-350 exhibited the highest air content of 5.5%, which was associated with the lowest particle packing density calculated for this mixture (0.74), while the mixture containing GS-275 showed a low air content of 4.6% that corresponded to a high particle packing density of 0.78. It should be noted that this air was entrapped air, and was generated by the PCE-based HRWRA used in the mix design. A defoaming agent was not used to reduce the entrapped air.

Fig. 6 presents the f'_c of the three mixtures in Series I compared to the reference mixture after different ages of NC and 2 days of HC. The figure also provides the corresponding packing-density values for the four mixtures. In general, the mixtures with GS exhibited lower f'_c compared to the reference mixture, regardless of age and curing conditions. For example, the 91-day f'_c of NC for the reference, 0QS/100GS-225, 0QS/100GS-275, and 0QS/100GS-350 mixtures were 182, 127, 157, and 128 MPa, respectively. The corresponding values after 2 days of HC were 204, 164, 182, and 153 MPa, respectively. The QS used in the present work performed well in producing the UHPC, mainly because of its very high silica content. On the other hand, the decrease in f'_c can be due to decreased packing densities in the mixtures incorporating GS (0.75, 0.78, and 0.76 for 0QS/100GS-225, 0QS/100GS-275, and 0QS/100GS-350, respectively) compared to the reference (0.79). In fact, when a compressive force is applied, the shear and tensile stresses develop at the interfaces between the aggregates and

Table 3
Fresh-concrete properties.

Property	Reference	Series I (100% replacement of QS with GS with different PSDs)			Series II (QS replacement with GS with optimum granulometry (d_{50} = 275 µm)	
		0QS/100GS-350	0QS/100GS-275	0QS/100GS-225	50QS/50GS	0QS/100GS
Slump flow, mm	190	175	210	170	200	210
Air void, %	3.8	5.5	4.6	5.2	4.3	4.6
Unit weight, kg/m^3	2363	2292	2297	2300	2306	2297
Concrete temperature, °C	32	32	31	31	32	31

cement paste (transition zone), forming small cracks approximately proportional in size to the maximum aggregate diameter [28]. With regard to GS, the particles can measure 630 μm in length according to the sieving test, but the actual length can be up to 1.0 mm (Fig. 2 right), which tends to have more cracking potential under same loading or lower strength capacity. Moreover, the lower strength can be related to the GS particle shapes, which are rough, elongated, and flattened compared to the rounded surfaces of the QS particles. The strength reduction related to GS replacement can be also due to the lower adhesion between cement and GS as compared to cement and QS (higher absorption) [19]. Another explanation for decrease in the f'_c is the increase in the air content due to lower particle packing density. Fig. 7 shows the influence of increasing both the air content and particle packing density on the f'_c. When the packing of the system is improved, the air content decreases, leading to enhanced compressive strength of the concrete mixture.

The results of the three mixtures containing GS in Series I demonstrate that 0QS/100GS-275 had the highest packing density (0.78), which is very close to that of the reference (0.79). The workability properties of this concrete (mini-slump flow value = 210 mm) were better than that of the reference mixture (about 10% higher). The f'_c results measured for 0QS/100GS-275 were also the best among the three mixtures in Series I containing GS. This concrete exhibited f'_c values at 91 days of NC and 2 days of HC of 157 and 182 MPa, respectively (14% and 11% lower than the corresponding values reported for the reference mixture). Based on these results, the GS combination with a d_{50} of 275 μm (GS-275) will be discussed further in the following section as replacement for the various QS contents in the UHPC.

4.3. Replacement of quartz sand with optimum glass sand

Different contents (0%, 50%, and 100%) of GS-275 (optimized in the previous section) were used to replace QS in the conventional UHPC, and their relevant effects on workability, mechanical microstructure, and durability (ASR) properties were investigated through the reference, 50QS/50GS, and 0QS/100GS mixtures, respectively.

4.3.1. Fresh properties

Table 3 presents the fresh properties, including mini-slump flow, unit weight, air content, and concrete temperature, of 50QS/50GS and 0QS/100GS compared to the reference mixture. The mini-slump flow diameters were found to slightly increase at higher GS contents: 190, 200, and 210 mm for the reference, 50QS/50GS, and 0QS/100GS mixtures, respectively, as illustrated in Fig. 8. This a slight improvement was due replacing QS particles with the GS particles of low water absorption and smooth surface. Again, the use of PCE-based HRWRA without a defoaming agent resulted in higher air content (3.8–4.6%). A slight increase (0.5–0.8%) in the air content was noticed with the addition of 50% and 100% GS compared to the reference concrete. The increase in air content was also due to low packing density of the granular materials when incorporating GS particles.

4.3.2. Compressive strength

Fig. 8 gives the f'_c after 1, 7, 28, 56, and 91 days of NC and 2 days of HC for the reference, 50QS/50GS, and 0QS/100GS mixtures. In general, the f'_c results obtained after 2 days of HC were higher (11% vs. 14%) than those obtained after 91 days of NC, regardless of the QS replacement ratio. This was due to the higher pozzolanic reaction of the SF in the UHPC mixture, which can be activated by high temperature. This pozzolanic reaction led to a denser microstructure of C-S-H, and therefore, faster strength development.

The f'_c values for 50QS/50GS were very close to that of the reference mixture. The f'_c values for the reference mixture at 91 days of NC and 2 days of HC were 182 and 204 MPa, respectively. The corresponding f'_c values of 50QS/50GS were 171 and 196 MPa, respectively (only 6% and 4% reductions, respectively). The f'_c of the UHPC containing 100% GS replacement showed a quite large reduction of 14% and 11% at 91 days of NC and 2 days of HC, respectively, compared to the reference mixture. Despite this reduction, it exhibited strength higher than the 150 MPa required for classification as UHPC. It reached 157 and 182 MPa after 91 days of NC and 2 days of HC, respectively. As explained earlier, the strength reduction related to GS replacement can be due to the rough, elongated, and flattened nature of the GS particles. The low packing density values of granular materials incorporated in the GS-containing UHPC mixtures (50QS/50GS and 0QS/100GS of 0.785 and 0.780, respectively) compared the reference mixture (0.793) were attributed to the high air contents of the former two concrete mixtures, and consequently to the decrease in the mechanical strength.

4.3.3. Alkali–silica reaction

The limited use of GS in concrete is due to uncertainty about damaging expansion that might be caused by ASR between the high-alkali pore water in cement paste and the reactive silica in

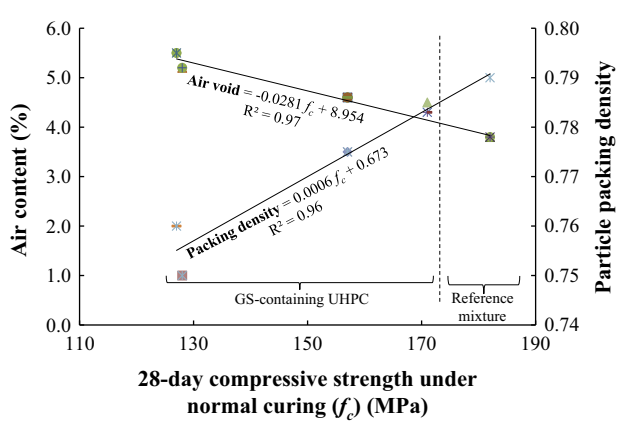

Fig. 7. Influence of air content and particle packing density on compressive strength for UHPC mixtures made with glass sand (GS) of different particle-size distributions (PSDs).

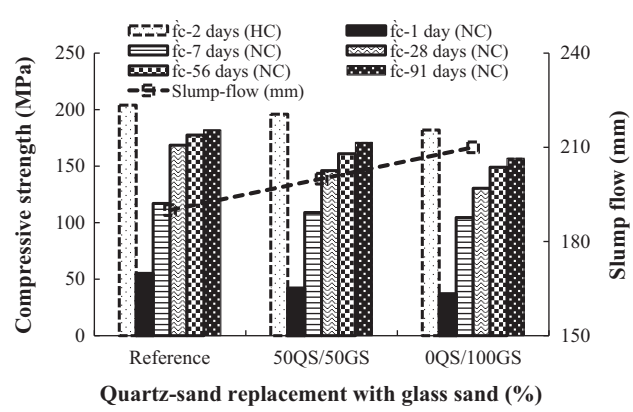

Fig. 8. Effect of quartz-sand replacement with glass sand (d_{50} = 275 μm) on compressive strength after different ages under normal (NC) and hot-curing (HC) conditions.

GS. For this reason, ASR expansion was assessed for 50QS/50GS. The accelerated ASR test was performed according to ASTM C1260 [46]. Fig. 9 provides the variations of expansion due to accelerated ASR with time up to 16 days. The maximum expansion at 16 days was 0.03%, which was less than (about one-third) the limit specifying the "innocuous behavior" (0.10%). This low expansion was obtained, however, the type HS cement used had higher alkali content [equivalent alkali (Na_2O_{eq}) = 0.9% (Table 1)]. The low ASR expansion for the UHPC containing GS can be attributed to the fact that the d_{max} of the GS particles used was smaller than 1 mm (630 μm). GS with such smaller particles produces C-S-H by pozzolanic reaction instead of ASR gel. Indeed, when the particles are slightly less than 1 mm a nonexpansive local ASR gel forms around the particles, which leads to better bonding between the particles and cement paste [22]. The low ASR expansion can also be explained by the very low w/b used for the UHPC (0.189), which does not provide enough moisture to initiate the reaction. This conclusion coincides with Vernet (2003), indicating that this UHPC is not susceptible to ASR due to its high silica-fume content and low permeability [48].

4.3.4. Microstructure analysis

The samples from the reference mixture after HC treatment and 50QS/50GS concretes after completion of the ASR test were also prepared for microstructure analysis under scanning electron microscope (SEM). All of the samples were epoxy impregnated, polished, and carbon coated to facilitate SEM analysis. Fig. 10 is a backscattering-scanning-electron (BSE) image of the reference mixture (A,B) and 50QS/50GS (C,D). Because of the low w/b, a large amount of unreacted cement, QP, and SF particles can be seen in the image. No visible capillary pores and cracks can be found, as well as portlandite ($Ca(OH)_2$) crystals. The UHPC was designed with close packing density and the use of pozzolanic mineral admixtures [49]. Therefore, it has very low porosity that is especially continuous. Entrained or entrapped spherical air pores were also observed in the UHPC matrix. Most of these pores were formed as a side effect of the superplasticizer used. Some of the black dots in Fig. 10 are probably the fingerprints of particles when the concrete was crushed. The figure clearly shows that the interfacial transition zone (ITZ) of the reference mixture was very thin or even nonexistent (Fig. 10).

Fig. 10 (C, D) reveals no ASR gel or microcracking ring around the GS particles. These results indicate that there should be no concern about ASR problems with the concrete containing GS. Free water must be present in order for ASR to occur in any concrete.

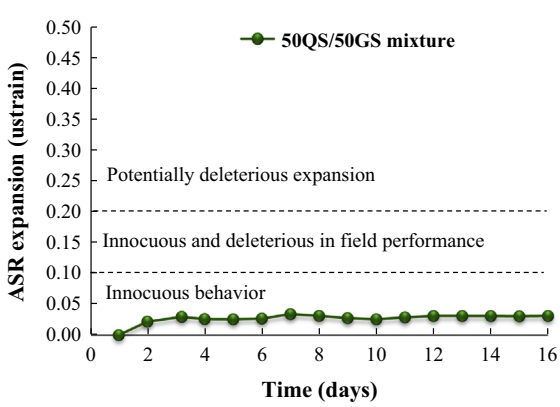

Fig. 9. Variations in expansion due to accelerated alkali–silica reaction (ASR) with time for 50QS/50GS according to ASTM C 1260.

Given the low permeability of this UHPC, it is unlikely that ASR would be an issue when GS is used

4.3.5. Cost analysis

Table 2 presents the normalized *cost index* (ratio between a given mixture's cost to the cost of the reference mixture) for all tested UHPC mixtures. This cost includes the cementitious materials and excludes the cost of steel fibers. Fig. 11 presents the relationship between the normalized *cost index* and 2-day HC f'_c obtained for all UHPC mixtures containing GS-275. The replacement of QS by GS (up to 50% replacement) led to a slight decrease in the f'_c followed by remarkable decrease thereafter. The percentage of the decrease in the f'_c at 50% and 100% replacement ratios were 4% and 11%, respectively. The corresponded reductions in the *cost index* values were 8% and 15%, which were found to be greater than the reductions in the strength. In addition, the transportation cost of materials (was not considered in the cost analysis) could also be reduced when using locally available GS in the production of UHPC.

An intensive effort to replace the crystalized QS of the very fine particles (150–600 μm) by another safe and healthy material is demanded by the Environment Canada and the International Agency for Research on Cancer. The current research offers the amorphous GS as an alternative, safe, and healthy material to replace the QS.

5. Conclusions

Based on the findings herein, the following conclusions can be drawn:

- The compressible packing model (CPM) in [39,40] can be applied on different glass sands of varying particle-size distributions to obtain final glass sand with an ideal particle-size distribution curve and optimum packing density using unitary, binary, and ternary combinations.
- Glass sand with an ideal particle-size distribution curve [mean-particle diameter (d_{50}) of 275 μm (GS-275)] was obtained in this research project. The glass sand (as total replacement of QS) can increase workability (10% higher), but with compressive strength less than 13% compared to the reference UHPC.
- Low packing density of granular materials incorporated in a UHPC mixture can be a result of high air content in the mixture and this negatively affects the mechanical strength.
- An optimum UHPC mixture can be designed with 50% glass-sand replacement of quartz sand. This mixture can deliver approximately similar flowability and compressive strength properties in comparison to the reference concrete.
- Incorporating 50% glass sand as quartz-sand replacement can yield a UHPC with a very dense microstructure and without any expansion from alkali–silica reaction. The results show that no alkali–aggregate reaction products are developed locally and have no negative influence on durability. This behavior is due to the UHPC's very low permeability, which prevents alkali ingress.
- Glass sand can be efficiently used to produce UHPC and eliminate the need for quartz sand, yielding a cost-effective and environmentally friendly solution.

Acknowledgments

The SAQ Industrial Chair on Valorization of Glass in Materials funded this research. The authors gratefully acknowledge this support. The authors also would like to thank Dr. Thierry Sedran and Dr. Ahmed Omran for their advices.

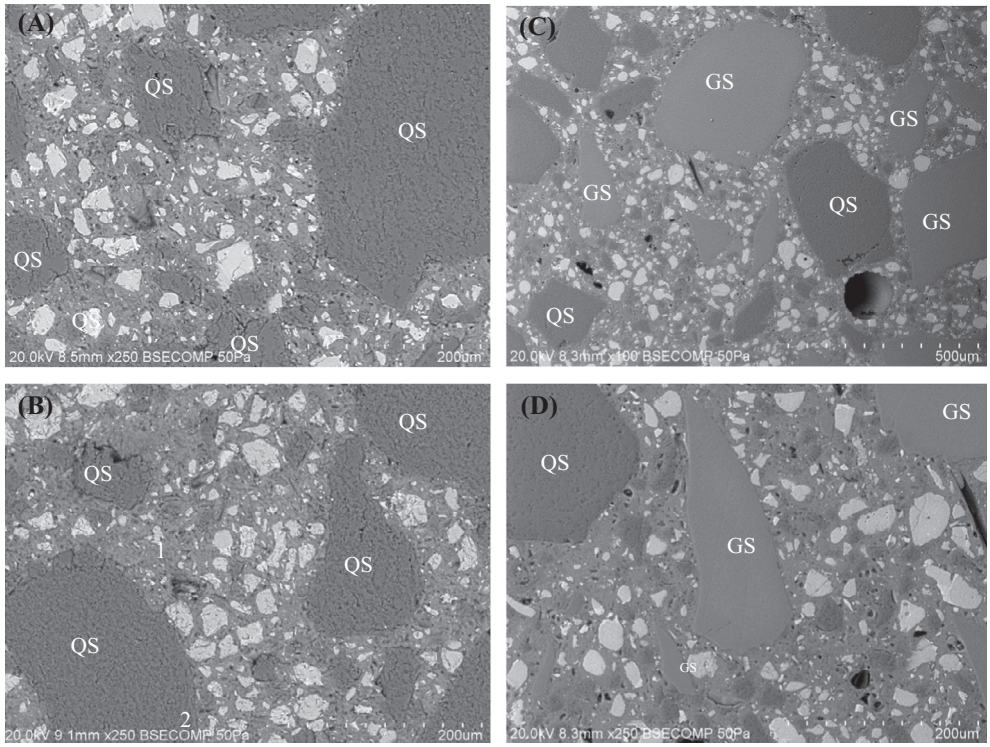

Fig. 10. BSE/SEM images for the reference mixture (A,B) and 50QS/50GS (C,D).

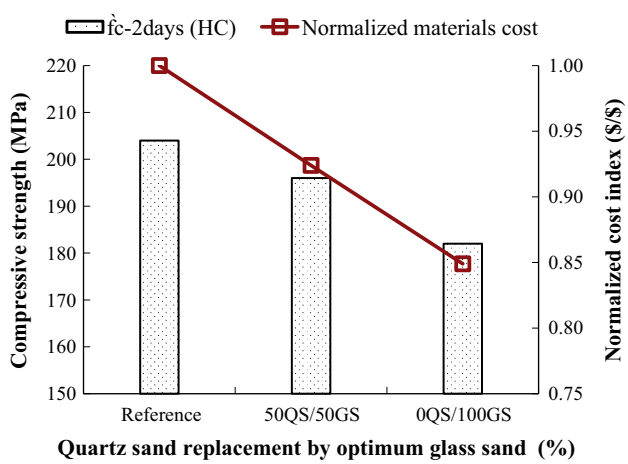

Fig. 11. Relative material price normalized to reference mixture and the 2-day compressive strength obtained under hot curing for UHPC containing optimum GS.

References

[1] A. Shayan, A. Xu, Value-added utilisation of waste glass in concrete, Cem. Concr. Res. 34 (1) (2004) 81–89.
[2] FEVE. Collection for recycling rate in Europe. The European Container Glass Federation (http://www.feve.org/FEVE-STATIS-2013/Recycling-2011-Glass-coll.html date accessed: Sept. 11, 2013).
[3] H. Du, K.H. Tan, Concrete with recycled glass as fine aggregates, ACI Mater. J. 111 (1) (2014) 47–58.
[4] J.R. Wright, C. Cartwright, D. Fura, F. Rajabipour, Fresh and hardened properties of concrete incorporating recycled glass as 100% sand replacement, J. Mater. Civ. Eng. 26 (10) (2014) 04014073.
[5] Y. Shao, T. Lefort, S. Moras, D. Rodriguez, Studies on concrete containing ground waste glass, Cem. Concr. Res. 30 (2000) 91–100.
[6] T.D. Dyer, R.K. Dhir, Chemical reactions of glass cullet used as cement component, J. Mat. Civil Eng. 13 (6) (2001) 412–417.
[7] C. Shi, Y. Wu, C. Riefler, H. Wang, Characteristic and pozzolanic reactivity of glass powders, Cem. Concr. Res. 35 (2005) 987–993.
[8] N. Neithalath, Quantifying the effects of hydration enhancement and dilution in cement pastes containing coarse glass powder, Adv. Concr. Technol. 6 (3) (2008) 397–408.
[9] N. Schwarz, H. Cam, N. Neithalath, Influence of a fine glass powder on the durability characteristics of concrete and its comparison to fly ash, Cem. Concr. Compos. 30 (6) (2008) 486–496.
[10] J.A. Jain, N. Neithalath, Chloride transport in fly ash and glass powder modified concretes-influence of test methods on microstructure, Cem. Concr. Compos. 32 (2) (2010) 148–156.
[11] A.M. Matos, J. Sousa-Coutinho, Durability of mortar using waste glass powder as cement replacement, Constr. Build. Mater. 36 (2012) 205–215.
[12] A. Khmiri, M. Chaabouni, B. Samet, Chemical behavior of ground waste glass when used as partial cement replacement in mortars, Const. Build. Mat. 44 (2013) 74–80.
[13] M. Carsana, M. Frassoni, L. Bertolini, Comparison of ground waste glass with other supplementary cementitious materials, Cem. Concr. Compos. 45 (2014) 39–45.
[14] J. Kim, J.H. Moon, J.W. Shim, J. Sim, H.G. Lee, G. Zi, Durability properties of a concrete with waste glass sludge exposed to freeze-and-thaw condition and de-icing salt, Constr. Build. Mater. 66 (2014) 398–402.
[15] M. Mirzahosseini, K.A. Riding, Effect of curing temperature and glass type on the pozzolanic reactivity of glass powder, Cem. Concr. Res. 58 (2014) 103–111.
[16] H. Du, K.H. Tan, Transport properties of concrete with glass powder as supplementary cementitious material, ACI Mater. J. (2014). accepted for publication.
[17] W. Jin, C. Meyer, S. Baxter, Glascrete concrete with glass aggregate, ACI Mater. J. 97 (2) (2000) 208–213.
[18] Z.Z. Ismail, E.A. Al-Rashmi, Recycling of waste glass as a partial replacement for fine aggregate in concrete, Waste Manage. 29 (2) (2009) 655–659.
[19] S.B. Park, B.C Lee, J.H. Kim, Studies on mechanical properties of concrete containing waste glass aggregate, Cem. Concr. Res. 34 (12) (2004) 2181–2189.
[20] P. Turgut, E. S. Yahlizade, Research into Concrete Blocks with Waste Glass. World Academy of Science, Engineering and Technology, International Journal of Civil, Environmental, Structural, Construction and Architectural Engineering, 3(3), 2009.
[21] B. Taha, G. Nounu, Properties of concrete contains mixed colour waste recycled glass as sand and cement replacement, Constr. Build. Mater. 22 (5) (2008) 713–720.
[22] Idir R, Cyr M, Tagnit-Hamou A. Use of waste glass as powder and aggregate in cement-based materials. SBEIDCO – 1st Int Conf on Sust built Env Infr in Developing Countries ENSET, Oran Algeria 12–14 October 2009:109–116.
[23] Benoit. Fournier, Marc.-André. Bérubé, Alkali-aggregate reaction in concrete: a review of basic concepts and engineering implications, Can. J. Civ. Eng. 27 (2) (2000) 167–191, http://dx.doi.org/10.1139/l99-072.

[24] B. Topcu, A.R. Boga, T. Bilir, Alkali-silica reactions of mortars produced by using waste glass as fine aggregate and admixtures such as fly ash and LizC03, Waste Manage. 28 (5) (2008) 878–884.
[25] C. Polley, S.M. Cramer, R.V. de la Cruz, Potential for using waste glass in Portland cement concrete, J. Mater. Civ. Eng. 10 (4) (1998) 210–219.
[26] C.S. Lam, C.S. Poon, D. Chan, Enhancing the performance of precast concrete blocks by incorporating waste glass - ASR consideration, Cem. Concr. Compos. 29 (8) (2007) 616–625.
[27] P. Richard, M. Cheyrezy, Composition of reactive powder concretes, Cem. Concr. Res. 25 (7) (1995) 1501–1511.
[28] P. Richard, M. Cheyrezy, Reactive powder concretes with high ductility and 200–800 MPa compressive strength, ACI SP 144 (1994) 507–518.
[29] J. Dugat, N. Roux, G. Bernier, Mechanical properties of reactive powder concretes, Mater. Struct. 29 (1996) 233–240.
[30] N. Roux, C. Andrade, M. Sanjuan, Experimental study of durability of reactive powder concretes, J. Mat. Civil Eng. 8 (1) (1996) 1–6.
[31] O. Bonneau, M. Lachemi, E. Dallaire, J. Dugat, P.-C. Aïtcin, Mechanical properties and durability of two industrial reactive powder concretes, ACI Mater. J. 94 (4) (1997) 286–290.
[32] N. Soliman, A. Tagnit-Hamou, Study of rheological and mechanical performance of ultra-high-performance glass concrete. ACI SP-fib bulletin and FRC 2014 Joint ACI-fib Int Workshop. Fibre Reinforced Concrete: from Design to Structural Applications 2015:17.
[33] M. Schmidt, E. Fehling, Ultra-high-performance concrete: research, development and application in Europe, ACI SP 225 (2005) 51–77.
[34] T. Klemens, Flexible concrete offers new solutions, Concr. Const. 49 (12) (2004) 72.
[35] A. Tagnit-Hamou, N. Soliman. "Ultra-High Performance Glass Concrete and Method for Producing same," U.S. Patent Application. No. 61/806,083, file March 28, 2013, Accepted March 2014.
[36] P. Racky, Cost-effectiveness and Sustainability of UHPC. Proc. of the Int Symp on UHPC, Kassel, Germany 2004;13(15),797–805.
[37] Environment Canada, https://www.ec.gc.ca/default.asp?lang=en&n=FD9B0E51-1.
[38] Environment Canada, Health Canada. Screening assessment for the challenge. Report June 2013:7.
[39] F. De Larrard, Concrete Mixture Proportioning: A Scientific Approach London: Modern Concrete Technology Series, E&FN SPON, London, 1999.
[40] T. Sedran, F. de Larrard, Manuel d'utilisation de RENE-LCPC, version 6.1d, logiciel d'optimisation granulaire, Laboratoire Centrale des Ponts et Chaussées, 2000.
[41] P.-C. Aïtcin, Cements of yesterday and today–concrete of tomorrow, Cem. Concr. Res. 30 (9) (2000) 1349–1359.
[42] CAN/CSA A3001–13. Cementitious materials for use in concrete. 2013:15–39.
[43] ASTM C185. Standard Test Method for Air Content of Hydraulic Cement Mortar. ASTM International, West Conshohocken, PA. Developed by Subcommittee: C01.21, Book of ASTM Standards 2015; V 04.01: 4.
[44] ASTM C1437. Flow of Hydraulic Cement Mortar. ASTM International, West Conshohocken, PA. Developed by Subcommittee: C01.22, Book of ASTM Standards 2007; V 04.01: 2.
[45] ASTM C109. Standard test method for compressive strength of hydraulic cement mortars (using 2-in. or [50-mm] cube specimens). ASTM International, West Conshohocken, PA. Developed by Subcommittee: C01.27, Book of ASTM Standards 2016; V 04.01: 10.
[46] ASTM C1260. Standard Test Method for Potential Alkali Reactivity of Aggregates (Mortar-Bar Method). ASTM International, West Conshohocken, PA. Developed by Subcommittee: C09.26, Book of ASTM Standards 2014; V 04.02: 5.
[47] F.V. Muellera, O.H. Wallevika, K.H. Khayat, Linking solid particle packing of Eco-SCC to material performance, Cem. Concr. Compos. 54 (2014) 117–125.
[48] C. Vernet, "UHPC microstructure and related durability performance laboratory assessment and field experience examples". Proc., 2003 Int. Symp. on High Performance Concrete, Orlando, Fla, 2003.
[49] M. Cheyrezy, V. Maret, L. Frouin, Microstructural analysis of RPC (Reactive Powder Concrete), Cem. Concr. Res. 25 (7) (1995) 1491–1500.

Nancy A. Soliman. is member of the ACI International and Sherbrooke Local Chapters, and CRIB. She is a doctoral candidate in the Department of Civil Engineering, University of Sherbrooke, QC, Canada. Her research interest includes NDT, ultra-high-performance concrete, microstructure, and sustainable development.

Arezki Tagnit-Hamou. FACI and professor in the Department of Civil Engineering at the University of Sherbrooke (QC, Canada) heads the cement-and-concrete group and holds an industrial chair on the valorization of glass in materials. He serves on ACI Committees 130 (Sustainability of Concrete) and 555 (Concrete with Recycled Materials), and RILEM TC DTA. His research interests include alternative cementitious materials, physical chemistry and microstructure of cement and concrete and sustainable development.